ACS Catalysis

Research Article

pubs.acs.org/acscatalysis

Rhodium(III)-Catalyzed Annulation between *N*-Sulfinyl Ketoimines and Activated Olefins: C−H Activation Assisted by an Oxidizing N−S Bond

Qiang Wang,[†] Yingzi Li,[‡] Zisong Qi,[†] Fang Xie,[†] Yu Lan,[*,‡] and Xingwei Li[*,†]

[†]Dalian Institute of Chemical Physics, Chinese Academy of Sciences, Dalian 116023, People's Republic of China

[‡]School of Chemistry and Chemical Engineering, Chongqing University, Chongqing 400030, People's Republic of China

Supporting Information

ABSTRACT: C−H activation under redox-neutral conditions, especially by Rh(III) catalysis, has offered attractive synthetic strategies. Previous work in redox-neutral C−H activation relied heavily on the cleavage of oxidizing N−O and N−N directing groups, and cleavable N−S bonds have been rarely used, although they may offer complementary coupling patterns. In this work, *N*-sulfinyl ketoimines were designed as a novel substrate for the redox-neutral coupling with different activated olefins via a Rh-catalyzed C−H activation pathway. The coupling with acrylate esters afforded 1*H*-isoindoles with the formation of three chemical bonds around a quaternary carbon. Furthermore, the coupling with maleimides furnished pyrrolidone-fused isoquinolines. A broad scope of substrates has been established. The mechanism of the coupling with acrylates has been studied in detail by a combination of experimental and computational methods. This coupling proceeds via imine-assisted C−H activation of the arene followed by ortho C−H olefination to afford a Rh(III) olefin hydride intermediate which, upon deprotonation, may exist in equilibrium with a Rh(I) olefin species. Cleavage of the N−S bond occurs only after C−H olefination to generate a Rh(III) imide species. DFT studies indicated that the imide group can undergo migratory insertion to produce a Rh(III) secondary alkyl which isomerizes under the assistance of acetic acid to a Rh(III) tertiary alkyl that is prone to insertion of the second acrylate.

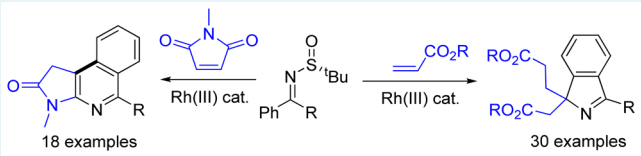

KEYWORDS: *C−H bond activation, Rh(III) catalyst, N−S bond cleavage, N-sulfinyl imine, olefin, isoindole*

INTRODUCTION

In the past several years, Rh(III)-catalyzed C−H activation of arenes has been increasingly explored, which allowed the development of a large number of important synthetic methods with high reactivity, selectivity, functional group tolerance, and broad applicability.[1] Building on the extensively studied Rh(III)-catalyzed C−H activation and coupling with various unsaturated partners under oxidative conditions using external oxidants,[2] there has been increasing interest in taking advantage of an internal oxidant or an oxidizing directing group. Pioneering work by Fagnou[3] and Glorius[4] utilized oxidizing N−O and N−N bonds as directing groups, and these C−H activation reactions proceeded with redox economy and high selectivity under relatively mild conditions.[5] Inspired by these seminal works, the N−N, N−O, and even C−N bonds in oximes,[6] hydrazines,[7] *N*-phenoxyamides,[8] *N*-oxides,[9] *N*-nitrosoanilines,[10] *N*-hydroxyanilines,[11] and *α*-ammonium acetophenones[12] have been designed and applied as viable oxidizing directing groups. Despite the progress, cleavage of a N−S directing group is highly rare.[13] This is likely due to the lower oxidizing potential of a N−S bond. Thus, the development of coupling systems for arenes bearing a cleavable N−S bond is of significant interest and may complement existing internal oxidizing systems.

While the concept of oxidizing DG is appealing, it is important to note that the substrate should be readily available and C−H activation reactions using external oxidants or using alternative substrates are poorly accessible. We reasoned that readily accessible *N*-sulfinylimines may serve this purpose, because the coordinating properties and polarity of the S═O bond may facilitate both C−H activation and N−S bond cleavage. Previously, C−H activation assisted by *N*-sulfonylimines or other N−S functionalities has been extensively explored.[14] However, only in one case was N−S cleavage involved (Scheme 1).[13] On the other hand, although the N−O bond in oxime ethers/esters may well act as an internal oxidizing DG, their couplings with olefins only afforded six-membered rings (Scheme 1).[15] We now report complementary reactivity of *N*-sulfinylimines in C−H activation and coupling with different olefins, leading to efficient construction of five- and six-membered heterocycles that are hardly accessible.

RESULTS AND DISCUSSION

Optimization Studies. We initiated our studies with the exploration of the reaction parameters of the coupling between benzophenone-derived *N-tert*-butylsulfinyl ketoimine ((*R*)-**1a**) and ethyl acrylate (**2a**) catalyzed by $[RhCp^*Cl_2]_2/AgSbF_6$ in DCE at 100 °C (Table 1). The coupling proceeded with poor efficiency when no additive was employed (entry 1). Introduction of HOAc (1.2 equiv) as an additive improved the GC yield to 39% (entry 2), and the coupled product **3aa** was

Received: October 14, 2015
Revised: February 8, 2016
Published: February 9, 2016

DOI: 10.1021/acscatal.5b02297
ACS Catal. 2016, 6, 1971−1980

Scheme 1. C−H Activation of Imines Bearing an Oxidizing DG

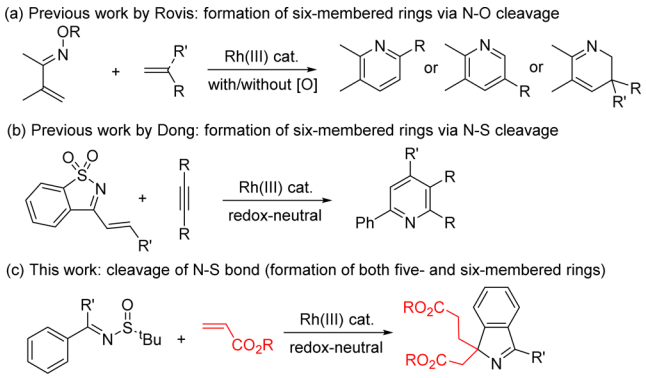

Table 1. Optimization Studies[a]

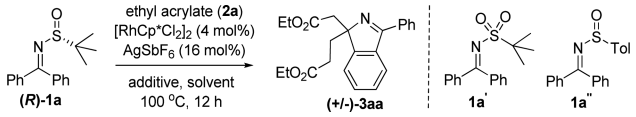

entry	additive (amt (equiv))	solvent	yield (%)[b]
1		DCE	<10
2	HOAc (1.2)	DCE	39
3	PivOH (1.2)	DCE	25
4	TFA (1.5)	DCE	<10
5	HOAc (1.2)	PhCl	30
6	HOAc (1.2)	DCM	35
7		DCE/HOAc (20/1)	73
8		DCE/HOAc (30/1)	81
9		DCE/HOAc (50/1)	56
10		DCE/HOAc (30/1)	69[c]
11	$Zn(OTf)_2$ (0.1)	DCE/HOAc (30/1)	92 (93)
12	$Zn(OTf)_2$ (0.3)	DCE/HOAc (30/1)	79
13	$Zn(OTf)_2$ (0.1)	DCE/HOAc (30/1)	N.D.[d]
14	$Zn(OTf)_2$ (0.1)	DCE/HOAc (30/1)	30[e]
15	AgOTf (0.1)	DCE/HOAc (30/1)	75
16	$Cu(OTf)_2$ (0.1)	DCE/HOAc (30/1)	50

[a]Reaction conditions: **1a** (0.2 mmol), **2a** (0.6 mmol), $[RhCp^*Cl_2]_2$ (4 mol %), $AgSbF_6$ (16 mol %), and additive in a solvent (3 mL) at 100 °C, sealed tube under N_2 for 12 h. [b]GC yield using mesitylene as an internal standard (isolated yield in parentheses). [c]$[RhCp^*(MeCN)_3](SbF_6)_2$ (8 mol %) was used as a catalyst. [d]Substrate **1a′** was used as the imine source. [e]Substrate **1a″** was used as the imine source.

fully characterized as a racemic 1*H*-isoindole, and the identity of one of its analogues has been unambiguously confirmed by X-ray crystallography (**3ed**; see Scheme 2).[16] Thus, three bonds were constructed around a quaternary carbon in a single step.[17] Other acid additives (TFA and PivOH) proved to be less efficient (entries 3 and 4). Further improvement was realized when HOAc was used as a cosolvent, and the optimal volumetric ratio of DCE to HOAc was found to be 30:1, which corresponds to 8 equiv of AcOH (entries 7−9), under which conditions the product was isolated in 81% yield. In contrast to in situ activation of the rhodium catalyst via chlroide abstraction, coupling using the preformed cationic complex $[RhCp^*(MeCN)_3](SbF_6)_2$ only gave inferior results (entry 10). To our delight, a high GC yield (92%) of **3aa** was secured when $Zn(OTf)_2$ (0.1 equiv) was further introduced as a coadditive (entry 11).[9b] Notably, the *N-tert*-butylsulfinyl group played an important role because switching this group to a *N-tert*-butylsulfonyl (**1a′**) or to a *N-p*-tolylsulfinyl (**1a″**) group gave poor or no reaction (entries 13 and 14). We also found that the reaction efficiency was somewhat lower when AgOTf or $Cu(OTf)_2$ was used as an additive (entries 15 and 16).

Substrate Scope. Having established the optimal conditions, we next explored the scope and limitations of this coupling system (Scheme 2). Imines derived from symmetric benzophenones bearing a para substituent coupled with ethyl acrylate in consistently high efficiency (**3ba−3fa**), where both electron-donating and -withdrawing para substituents are tolerated. Introduction of a *m*-Me group into both benzene rings caused the reaction to occur at the less hindered ortho site (**3ga**). 1- and 2-Naphthylphenone-derived sulfinylimines are also viable substrates, and the isolation of **3ia** in good yield indicates tolerance of steric hindrance associated with a 1-naphthyl group. A variety of unsymmetrically substituted imines also coupled in high selectivity, and the selectivity can be well dictated by the steric effects. Thus, with the introduction of a sterically more hindered ortho or meta substituent into one phenyl ring, C−H activation occurred at the more sterically accessible ring in high yield and with high site selectivity **3ja−3oa**. To examine the electronic preference of this coupling reaction, an electronically biased diarylimine was allowed to couple with ethyl acrylate. ^1H, ^{19}F, and ^{13}C NMR analyses of the product mixture (**3pa** and **3pa′**) revealed that the C−H activation occurred preferentially at the more electron rich ring. Indeed, this observation is consistent with the fact that essentially no desired reaction occurred for the imine derived from bis(*p*-(trifluoromethyl)phenyl)methanone. The imine can be extended to those of acetophenones, and such imines can be smoothly converted to the isoindole product in relatively lower yields (**3pa**, **3ra**), where the decrease of the reaction yield is ascribable to the higher tendency of hydrolysis (reduced steric protection). The acrylate coupling partner has also been extended to methyl, *n*-butyl, and benzyl acrylates, and couplings with these acrylates also tolerated various substituents in the imine substrate (**3ab−3hc**). In all cases, good to excellent yields were obtained.

Coupling with an Enone. To better define the scope of the olefin, ethyl vinyl ketone was applied as a direct anlogue. While enones may seem more reactive, the coupling afforded an indene in good yield under mild conditions.[18] This reaction likely proceeded via hydroarylation of the olefin to afford an alkylated intermediate followed by hydrolysis of the imine moiety; subsequent intramolecular aldol condensation furnished the final product.[18a]

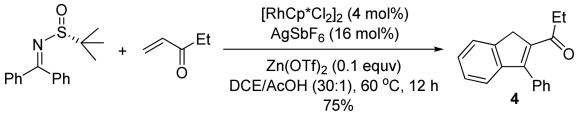

(1)

Coupling with Maleimides. To further define the scope of the olefin, we applied *N*-methylmaleimide as an activated olefin.[19] We reasoned that migratory insertion of an aryl group into this cyclic olefin should lead to an alkyl species that cannot undergo *β*-H elimination due to requirement of a syn-coplanar orientation of the H−C−C−Rh moiety. Therefore, different reactivity should be expected. Indeed, the coupling of **1a** with *N*-methylmaleimide afforded a pyrrolidone-fused isoquinoline, and a similar scope and regioselectivity of the imine substrate have been observed (Scheme 3). Notably, acetophenone-derived *N*-sulfinylimines reacted with equally high efficiency (**5i−q**). In nearly all cases, good to high yields have been obtained. It is noteworthy that, while maleimides have been used as a coupling

DOI: 10.1021/acscatal.5b02297
ACS Catal. 2016, 6, 1971−1980

Scheme 2. Scope of Synthesis of 1*H*-Isoindoles[a,b]

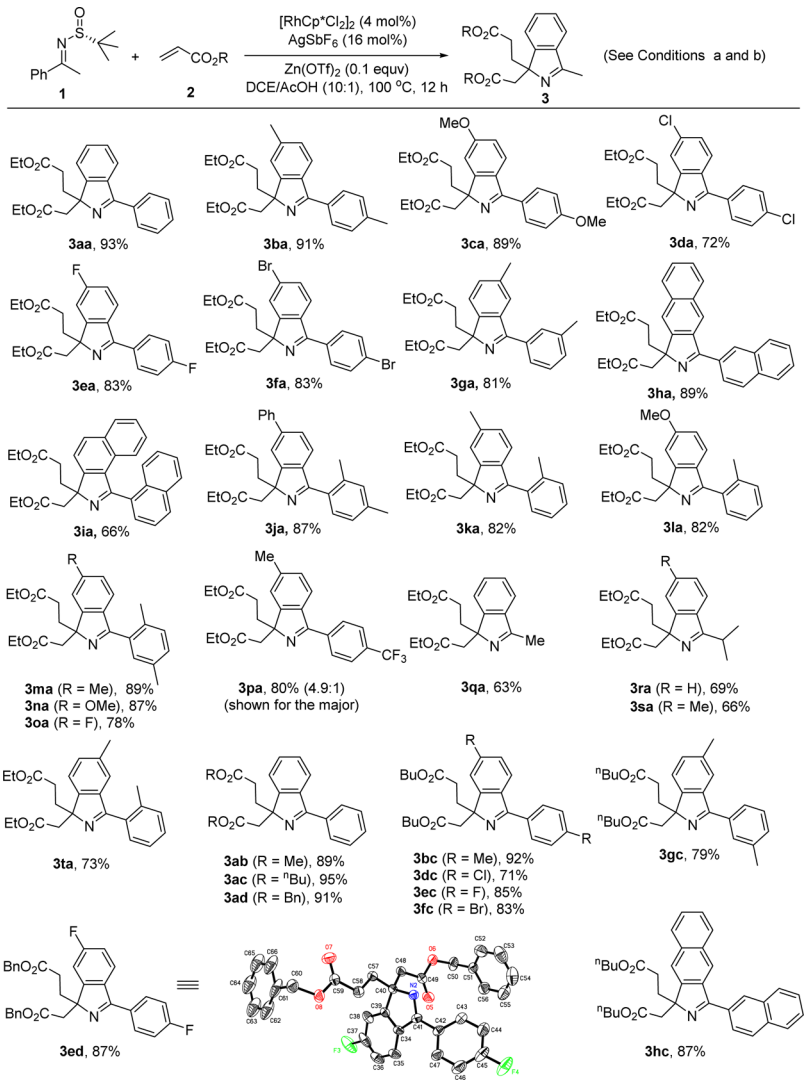

[a]Reaction conditions: imine (0.2 mmol), acrylate ester (0.6 mmol), $[RhCp^*Cl_2]_2$ (4 mol %), $AgSbF_6$ (16 mol %), $Zn(OTf)_2$ (0.1 equiv) in DCE/AcOH (3 mL, 30/1) at 100 °C for 12 h, sealed tube under N_2. [b]Isolated yield after column chromatography.

partners in C−H activation reactions, in all cases they acted as either a C_1 source or a simple π bond,[19] and coupling with loss of an oxygen atom has not been reported.

Derivatization of a Coupled Product. To briefly demonstrate the synthetic usefulness of the fused isoquinoline product, heterocycle **5h** was derivatized. Simple treatment of **5h** with $NaBH_4$ in the presence of $ZnCl_2$ afforded a pyrrole-fused isoquinoline (**6**) in 78% yield (eq 2). This extended aromatic system may exhibit valuable biological activities.[20]

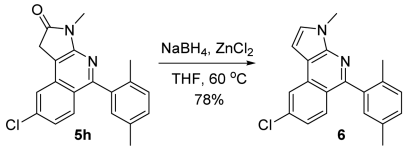

(2)

Experimental Mechanistic Studies: H/D Exchange and Kinetic Isotope Effects. A series of mechanistic studies have been performed to probe the reaction mechanism (Scheme 4). To explore the C−H activation process, H/D exchange was performed for **1a** in DCE-CD_3COOD in the absence of any olefin (Scheme 4a). ^{1}H NMR analysis revealed 15% deuteration at the ortho positions of the para-substituted benzene ring, suggestive of reversible C−H activation in the absence of any olefin. Moreover, ^{1}H NMR analysis of the coupled product obtained from **1a**-d_{10} and ethyl acrylate (DCE-AcOH) revealed essentially no H/D exchange in any alkyl group and only **3aa**-d_9 was obtained. On the other hand, when the coupling of **1a** with **2a** was performed in DCE-CD_3COOD, no deuterium was incorporated into any phenyl ring, which collectively points to irreversible C−H activation in the presence of an olefin substrate. Importantly, H/D exchange was observed at both α-methylene positions (Scheme 4a). In one of the methylene groups, both protons are deuterated to the same extent (72% D). However, in the other α-methylene, only one of the protons was partially deuterated (20% D). Control experiments confirmed that the deuteration did not originate from post-coupling H/D exchange. These data also cast light on details of the mechanism (vide infra). To further probe the C−H activation process, KIE experiments have been carried out. ^{1}H NMR analyses of the product mixture obtained from an intramolecular competition using imine **1a**-d_5 revealed that the

DOI: 10.1021/acscatal.5b02297
ACS Catal. 2016, 6, 1971−1980

Scheme 3. Scope of the Coupling with Maleimides[a,b]

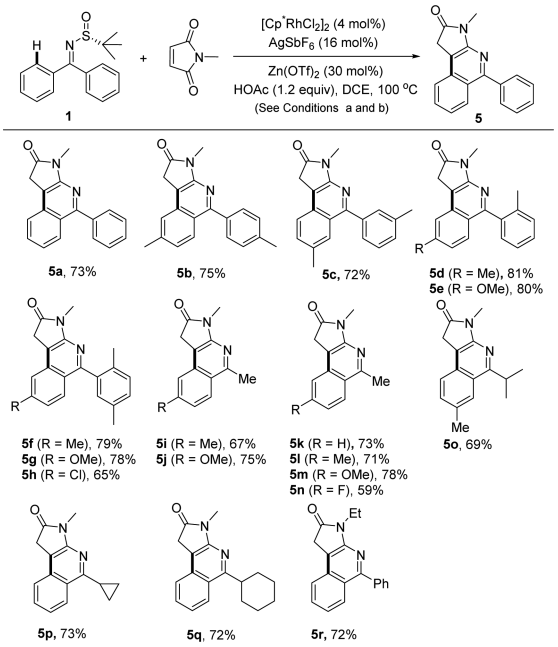

[a]Reaction conditions: imine (0.2 mmol), maleimide (0.3 mmol), $[RhCp^*Cl_2]_2$ (4 mol %), $AgSbF_6$ (16 mol %), $Zn(OTf)_2$ (0.3 equiv), AcOH (0.24 mmol), DCE/AcOH (3 mL) at 100 °C for 12 h, sealed tube under N_2. [b]Isolated yield after column chromatography.

C_6H_5 group reacts preferentially with a k_H/k_D value of 3.0 (Scheme 4b). In addition, KIE measurements using an equimolar mixture of **1a** and **1a**-d_{10} gave k_H/k_D = 2.3. These data consistently suggest that C−H activation is likely involved in the turnover-limiting step.

Intermediacy of an Olefinated Imine. To probe whether the reaction proceeded via initial C−H olefination, olefinated imine **7** was prepared as a *Z*/*E* mixture and was subjected to the standard conditions. However, it failed to undergo any conversion (Scheme 4c). We reasoned that it remains a possible intermediate because imine **7**, generated via *β*-H elimination, is accompanied by a Rh(III) hydride species which could exist in equilibrium with a Rh(I) species upon deprotonation, and it is the Rh(I) olefin or the Rh(III) hydride species that gave activity. Thus, we reasoned that by borrowing the transient Rh(I) or Rh(III) species generated in situ from the coupling of **1a** with ethyl acrylate, intermediate **7** could be converted. Indeed, reaction of a mixture of **7**, **1a**, and ethyl acrylate afforded **3aa** in a yield that exceeded 100% if based on the amount of **1a** (together with some benzophenone byproduct, Scheme 4d). Direct evidence was obtained using a Rh(I) catalyst. The coupling of **7** with ethyl acrylate catalyzed by $[RhCp^*(C_6Me_6)]$ afforded product **3aa** in 60% yield (Scheme 4e). In contrast, no coupling occurred when **1a** and **2a** were allowed to react using this Rh(I) catalyst. Furthermore, reaction of *n*-butyl acrylate with a mixture of **7** and **1a** afforded the mixed ester product **8** together with the homoester **3ac** in a 2:1 ratio (Scheme 4f, GC-MS analyses). To gain further mechanistic details, we relied on DFT studies.

General Remarks on DFT Studies. All DFT calculations were carried out using the GAUSSIAN 09[21] series of programs. The density functional B3-LYP[22] with a standard 6-31g* basis set (LANL08(f) basis set for Rh) was used for geometry optimizations. The M11-L[23] functional, proposed by Truhlar et al., was used with a 6-311+g* basis set (LANL08(f) basis set for Rh) to calculate the single-point energies because it was envisaged that this strategy would provide greater accuracy with regard to the energetic information.[9b,24] The solvent effects were considered by single-point calculations on the gas-phase stationary points with the SMD[25] solvation model. The energies presented in this paper are the M11-L calculated Gibbs free energies in 1,2-dichloroethane solvent with B3-LYP calculated thermodynamic corrections.

Possible Mechanistic Pathways. As shown in Scheme 5, on the basis of these experimental data, several possible pathways have been taken into account for the coupling between **1a** and **2a** as a model for theoretical studies at the DFT level. These four pathways begin with Rh(III) acetic acid complex **A**, which is followed by cyclometalation of imine **1a** to generate the rhodacyclic intermediate **B**. In pathway a (blue pathway), the Rh−C(aryl) bond of the common intermediate B is proposed to undergo migratory insertion into ethyl acrylate **2a** to generate the Rh(III) alkyl intermediate **C**, which is expected to undergo *β*-H elimination to afford the Rh(III) hydride **D**. As discussed

Scheme 4. Mechanistic Studies

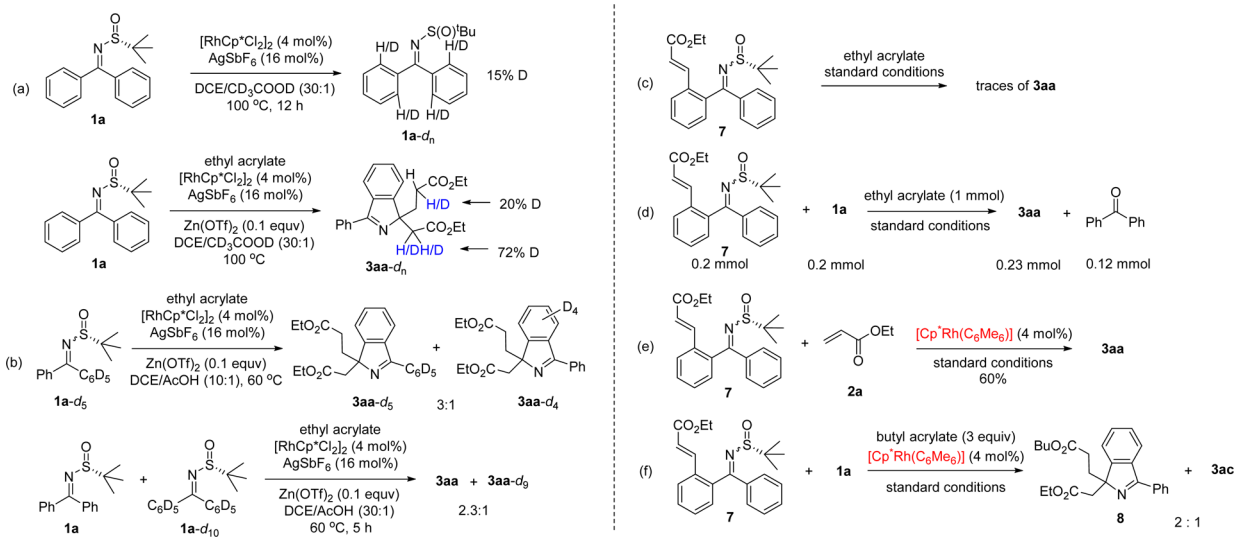

DOI: 10.1021/acscatal.5b02297
ACS Catal. 2016, 6, 1971−1980

Scheme 5. Possible Mechanistic Pathways for the Coupling of Imine 1a with Olefin Acrylate 2a (in the Circle) and a Likely Mechanism for the Coupling with a Maleimide (outside the Circle)

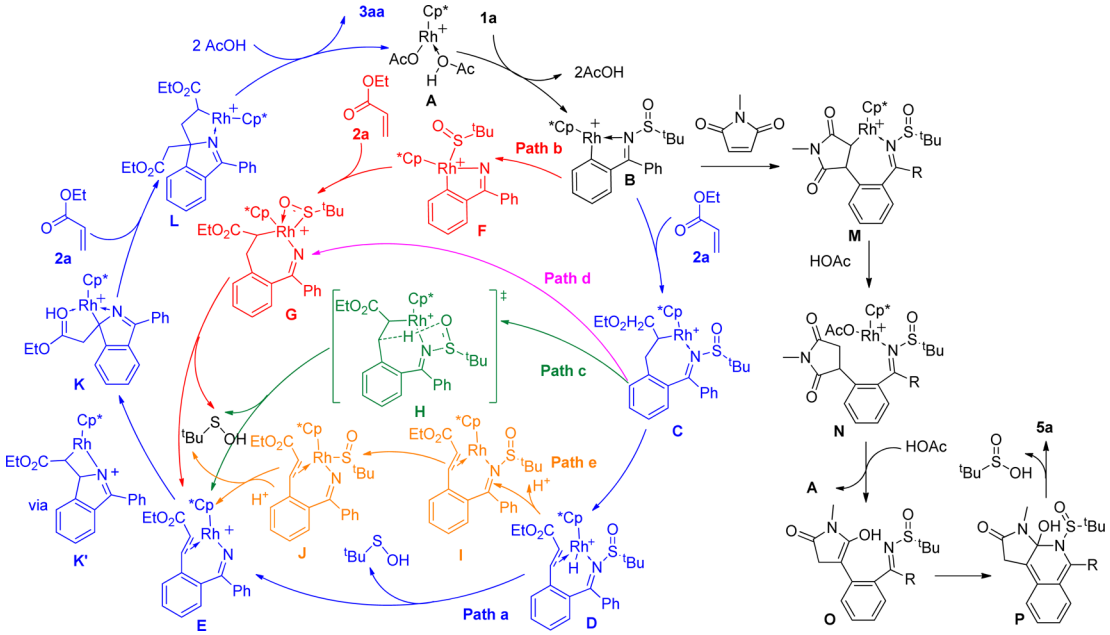

above, hydride species **D** may exist in equilibrium with the corresponding Rh(I) olefin intermediate **D′**. An intramolecular deprotonation of the Rh−H in **D** by the sulfinyl oxygen may take place with concomitant N−S bond cleavage to give intermediate **E** by releasing one molecule of ^{t}BuSOH. As discussed above, hydride species **D** also may exist in equilibrium with the corresponding Rh(I) olefin intermediate **I** (pathway e). The following intermolecular oxidative addition with an N−S bond in complex **I** would generate Rh(III) intermediate **J**. Protonolysis of intermediate **J** would release one molecule of ^{t}BuSOH and generate the same intermediate **E**. The transformation of intermediate **C** to intermediate **E** might also occur in a concerted fashion via the proposed transition state **H** (pathway c, green). Subsequently, migratory insertion of the imide group in Rh(III) imide intermediate **E** generates the Rh(III) alkyl intermediate **K′**, which further isomerizes to the Rh(III) alkyl intermediate **K** via a formal rhodium shift. Insertion of the second molecule of ethyl acrylate then takes place to give intermediate **L**, which is protonolyzed by acetic acid to release the final product **3a** with the regeneration of the active catalyst **A**. Although our experimental studies suggested the intermediacy of olefinated imine **7** and suggested that the C−H olefination occurs prior to the cleavage of the N−S bond, pathway b (red line) was still examined for comparisons. In this pathway, N−S oxidative addition of the intermediate **B** occurs prior to C−H olefination to afford the putative Rh(V) imide species **F**, the Rh−C(aryl) bond of which might then undergo migratory insertion into ethyl acrylate to form the Rh(V) intermediate **G**. Followed by intramolecular (or intermolecular) deprotonation, the common intermediate **E** could also be reached. Alternatively in pathway d (purple line), the N−S oxidative addition might occur at the stage of intermediate **C** to produce the intermediate **G**.

Plausible Mechanism of the Coupling with Maleimides. In line with the coupling with acrylates, the coupling with maleimides (Scheme 5, outside the circle) likely involves a Rh(III) alkyl species **M** that undergoes protonolysis to furnish intermediate **N**. Subsequent dissociation of the imine ligand releases the active Rh(III) catalyst **A**. The resulting hydroarylated intermediate is proposed to undergo 6π electrocyclization in its enol form (**O**) to provide the dearomatized intermediated **P**. Elimination of *tert*-butylsulfinic acid furnishes product **5a**. In this coupling reaction, the $Zn(OTf)_2$ additive likely facilitates the keto−enol tautomerization.

C−H Activation Process. To better understand the mechanism of the coupling with acrylates, all four of these possible pathways have been evaluated by using DFT calculations. The free energy profiles for the C−H activation step of the rhodium-catalyzed annulation between *N*-sulfinylketoimines and olefins are given in Figure 1. The energy of the solvento complex $Cp^*Rh^{III}(OAc)(AcOH)^+$ (**CP1**) was set to a relative zero value in the whole free energy profiles, and this complex could be readily generated from $[Cp^*RhCl_2]_2$ and $AgSbF_6$ via chloride abstraction and coordination of AcOH.[26] The dissociative ligand substitution between **CP1** and substrate **1a** forms the imine complex **CP3** with 4.1 kcal/mol exothermicity. The subsequent imine-directed, acetate-assisted C−H activation takes place via the transition state **TS3-4** (CMD mechanism) with an overall activation free energy of 27.7 kcal/mol, leading to formation of rhodacycle **CP4** and acetic acid. The reversibility established by DFT is in line with our observation of an imine substrate in the absence of any coupling partner (Scheme 4a).

The First Olefin Insertion and Cleavage of the N−S Bond. Starting from intermediate **CP4**, the free energy profiles of the first olefin insertion and the N−S bond cleavage for all of the plausible pathways are given in Figure 2. In pathway a (blue pathway), the coordination of **2a** forms olefin complex **CP5** with 7.2 kcal/mol endothermicity, and the subsequent olefin insertion occurs via transition state **TS5-6** with an activation free energy of 20.0 kcal/mol to reversibly produce the seven-membered rhodacycle **CP6**. Subsequent β-H elimination of **CP6** has been established via transition state **TS6-7**, and the barrier of this step is found to be 19.9 kcal/mol, which could be attributed to the strain and rigidity of the metallacycle in **CP6**. Subsequent intramolecular proton abstraction with concomitant N−S bond cleavage takes place via transition state **TS7-8**

DOI: 10.1021/acscatal.5b02297
ACS Catal. 2016, 6, 1971−1980

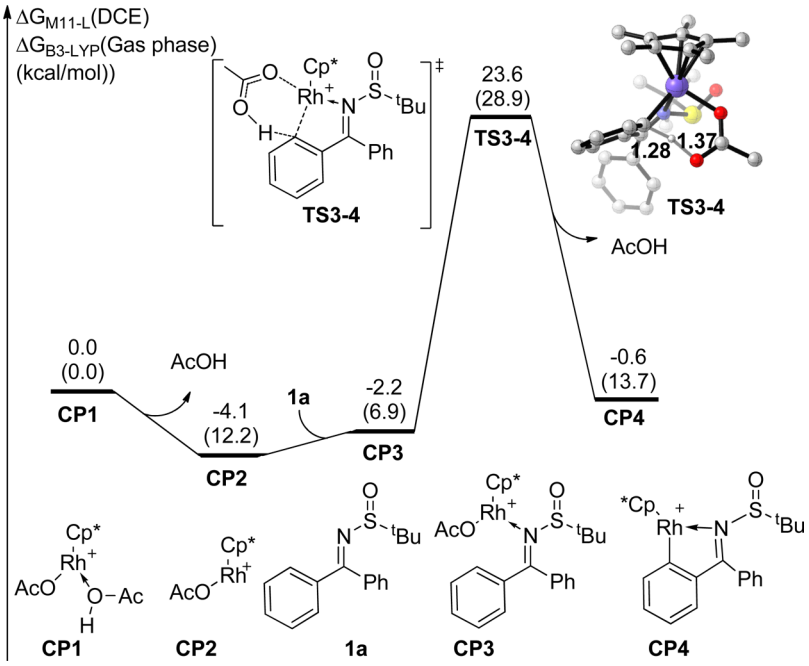

Figure 1. Free energy profiles for the *N*-sulfinylketoimine-directed acetate-assisted C−H activation of *N*-sulfinylketoimines. Values are given in kcal/mol and represent the relative free energies calculated by the M11-L method in DCE solvent. The values given in parentheses are the relative free energies calculated using the B3-LYP method in the gas phase. The values for the bond lengths given in the geometry information are reported in units of angstroms.

with a barrier of as low as 2.7 kcal/mol, and the imide complex **CP8** is formed irreversibly with the release of one molecule of *t*-BuSOH. We also considered the deprotonation of **CP7** (path e). As shown in Figure 2 (orange lines), when acetic acid is chosen as the proton acceptor, the proton transfer from **CP7** to acetic acid is exothermic. However, this barrier of this course is as high as 16.3 kcal/mol via transition state **TS7-11**. The relative free energy of **TS7-8** is 13.6 kcal/mol lower than that of **TS7-11**; therefore, path e is kinetically unfavorable.

We also managed to locate the transition state **TS6-8**, through which direct deprotonation of the alkyl C−H of **CP6** occurs to give **CP8**. However, the relative free energy of transition state **TS6-8** is 20.8 kcal/mol higher than that of the transition state **TS6-7**. Therefore, the proposed pathway c is unlikely. In the calculated energy profiles of pathway b, as shown in Figure 2 (red lines), the activation free energy for the N−S oxidative addition of **CP4** via transition state **TS4-9** was found to be 33.3 kcal/mol, leading to the formation of the Rh(V) sulfinyl intermediate **CP9** with 10.3 kcal/mol endothermicity. Furthermore, the activation free energy for the olefin insertion into the Rh−C bond in **CP9** via transition state **TS9-10** is also much higher than those for the olefin insertion, β-H elimination, and N−S bond cleavage in pathway a. Therefore, pathway b should also be explicitly ruled out due to unfavorable activation barriers. Analogously, the direct intramolecular N−S oxidative addition of **CP6** to generate **CP10** (pathway d) could not occur because the relative free energy of transition state **TS6-10** is 26.2 kcal/mol higher than that of transition state **TS6-7** in pathway a. On the basis of our theoretical calculations, we conclude that the N−S bond cleavage only occurs on the rhodium olefin hydride species, and the redox neutrality is maintained by the release of a *t*-BuSOH molecule.

Imide Migratory Insertion, Rhodium Migration, and the Second Olefin Insertion. As shown in Figure 3, with the formation of intermediate **CP8**, the intramolecular imide migratory insertion readily takes place via transition state **TS8-13** with a barrier of only 13.5 kcal/mol to irreversibly form intermediate **CP13**. The direct rhodium shift via transition state **TS13-16** to form intermediate **CP16** was found to be kinetically inaccessible because this bears a barrier as high as 39.5 kcal/mol. We also considered the β-H elimination and olefin reinsertion mechanism (green lines); however, the activation free energy for β-H elimination of complex **CP13** is also as high as 32.5 kcal/mol. Therefore, we deduce that acetic acid may promote this formal rhodium shift. As shown in Figure 3, the coordination of a molecule of acetic acid forms intermediate **CP14**, and the proton transfer from acetic acid to the enolate carbon moiety (protonolysis) takes place reversibly via transition state **TS14-15** with an overall activation free energy of 22.7 kcal/mol. Thus, further intramolecular deprotonation of the methine CH in intermediate **CP15** occurs readily and reversibly via transition state **TS15-16** to form isoindolyl rhodium intermediate **CP16**, which is 3.5 kcal/mol more stable than intermediate **CP13**, likely owing to the formation of a stable five-membered rhodacycle. Therefore, the acetic acid promoted rhodium shift is both kinetically and thermodynamically favorable. This mechanistic profile is also consistent with our experimental H/D exchange studies using CD_3COOD (Scheme 4b). The reversibility of this proton abstraction can readily give rise to deuteration of the two methylene protons α to the ester group. The coordination of the second ethyl acrylate to **CP16** is 17.1 kcal/mol uphill in free energy, which can be largely attributed to the excess coordination in intermediate **CP18**. The overall activation free energy for olefin insertion via transition state **TS18-19** is 24.7 kcal/mol. The intermediate **CP19** undergoes protonolysis by acetic acid to produce the N-bound isoindole complex **CP20**. Ligand substitution by an acetic acid released the active catalyst **CP1** together with the final product **3aa**. Notably, our theoretical

DOI: 10.1021/acscatal.5b02297
ACS Catal. 2016, 6, 1971−1980

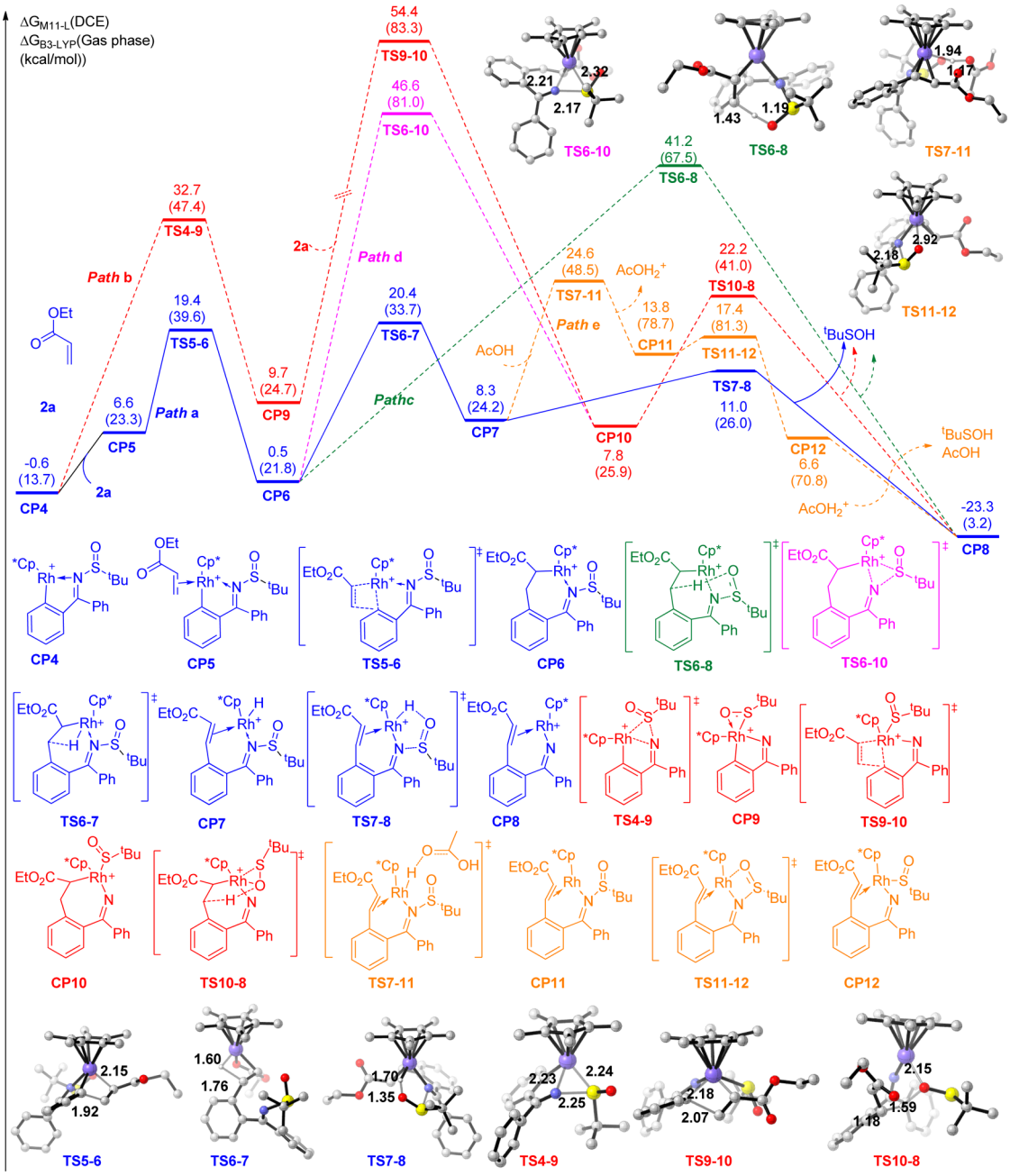

Figure 2. Free energy profiles for the first olefin insertion and the N−S bond cleavage in rhodium-catalyzed annulation between *N*-sulfinylketoimines and olefins. Values are given in kcal/mol and represent the relative free energies calculated by the M11-L method in DCE solvent. The values given in parentheses are the relative free energies calculated by using the B3-LYP method in the gas phase. The values for the bond lengths given in the geometry information are reported in units of angstroms.

data are in line with the fact that the coupling reaction will not stop at the stage of the monoinsertion of the olefin because comparisons between the energy profiles in Figure 3 and those in Figure 2 indicate that the kinetic barriers of the imide migratory insertion, rhodium migration, and the second olefin insertion are all lower than those in preceding processes.

Summary of DFT Studies. The rhodium-catalyzed annulation between *N*-sulfinyl ketoimines and acrylate has been examined in detail by DFT methods, and the most likely mechanism for this reaction has been outlined in pathway a, which involves four Rh(III) alkyl species. In this lowest energy pathway, the reaction proceeds with initial *N*-sulfinyl ketoimine directed, acetate-assisted C−H activation as a turnover-limiting step, followed by insertion of an olefin to afford the first alkyl species. *β*-H elimination generates a Rh(III) olefin hydride which is likely in equilibrium with a Rh(I) olefin intermediate. N−S bond cleavage occurs upon intramolecular abstraction of the Rh−H proton by the sulfinyl oxygen to afford an imide intermediate, which undergoes migratory insertion to give the second alkyl species. Isomerization of this secondary alkyl to the third, tertiary alkyl species has been examined in detail, and it is likely assisted by reversible protonolysis of the Rh−C(enolate) bond by AcOH. The fourth alkyl is generated from the insertion of the second molecule of olefin, and it is eventually protonolyzed by AcOH to afford the coupled product. Thus, the DFT data are in line with the experimental

DOI: 10.1021/acscatal.5b02297
ACS Catal. 2016, 6, 1971−1980

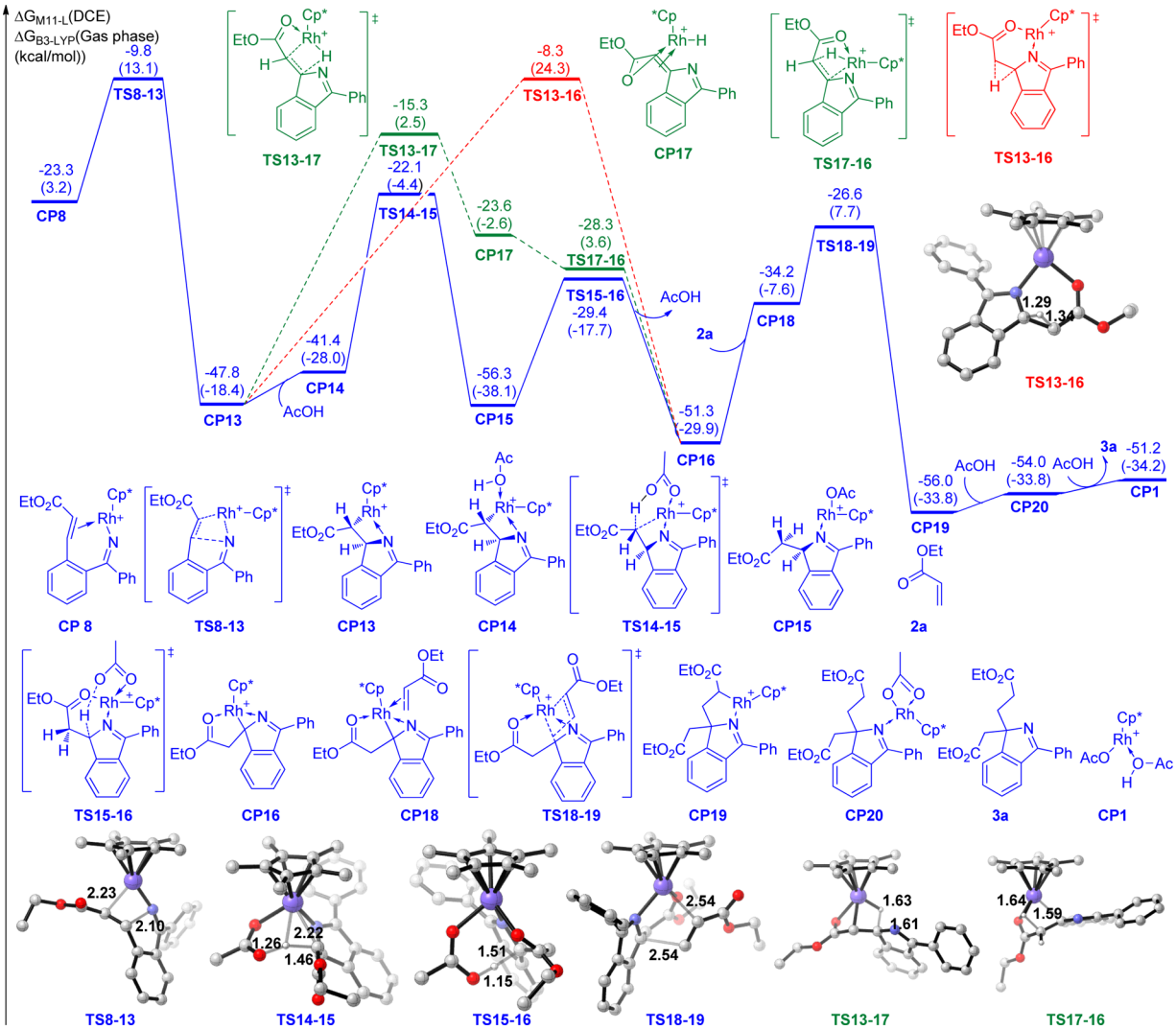

Figure 3. Free energy profiles for imide migratory insertion, formal rhodium shift, and protonolysis steps of the rhodium-catalyzed annulation between *N*-sulfinylketoimines and acrylates. Values are given in kcal/mol and represent the relative free energies calculated by the M11-L method in DCE solvent. The values given in parentheses are the relative free energies calculated by using the B3-LYP method in the gas phase. The values for the bond lengths given in the geometry information are reported in units of angstroms.

results in terms of intermediacy of an olefinated imine, KIE studies, H/D exchange experiments, and the observed 1:2 coupling with olefins. The DFT studies are also consistent with the absence of any diasteroselectivity, because the chiral sulfinyl group was already eliminated prior to the stereo-determining step.

■ CONCLUSIONS

We have designed *N-tert*-butylsulfinylimines as a novel arene substrate for the coupling with activated olefins with a N−S bond being an internal oxidant. The coupling with acrylates afforded substituted 1*H*-isoindoles as a result of C−H activation and 1:2 coupling, in which process three chemical bonds have been constructed around a quaternary center. The coupling with maleimides proceeded under similar conditions to afford pyrrolidone-fused isoquinolines. The mechanism of the coupling of *N-tert*-butylsulfinylimines with acrylates has been elaborated using a combination of experimental and theoretical methods. Our mechanistic studies revealed that the reaction proceeds via chelation-assisted C−H activation followed by *o*-C−H olefination to afford a Rh(III) olefin hydride intermediate that may exist in equilibrium with a Rh(I) olefin species upon deprotonation, and cleavage of the N−S bond occurs only after C−H olefination to generate a Rh(III) imide species. DFT studies also indicated that this imide group undergoes migratory insertion to produce a Rh(III) secondary alkyl, which isomerizes under the assistance of an acetic acid to give a Rh(III) tertiary alkyl that is prone to insertion of the second acrylate. These coupling systems extended the scope of arenes in Rh-catalyzed C−H activation, especially under redox-neutral conditions. Future studies are directed to asymmetric C−H activation/coupling reactions using this type of sulfinyl directing group.

■ ASSOCIATED CONTENT

Supporting Information

The Supporting Information is available free of charge on the ACS Publications website at DOI: 10.1021/acscatal.5b02297.

Experimental procedures, characterization data, ^{1}H and ^{13}C NMR spectra, and computational details (PDF)

Crystallographic data for **3ed** (CIF)

DOI: 10.1021/acscatal.5b02297
ACS Catal. 2016, 6, 1971−1980

AUTHOR INFORMATION

Corresponding Authors

*X.L.: e-mail, xwli@dicp.ac.cn; tel, +86-411-84379089.
*Y.L.: e-mail, lanyu@cqu.edu.cn; tel, +86-23-88288267.

Notes

The authors declare no competing financial interest.

ACKNOWLEDGMENTS

Financial support from the NSFC (Nos. 21272231, 21402190, and 21525208) and the Chinese Academy of Sciences are gratefully acknowledged.

REFERENCES

(1) (a) Colby, D. A.; Tsai, A. S.; Bergman, R. G.; Ellman, J. A. *Acc. Chem. Res.* **2012**, *45*, 814−825. (b) Kuhl, N.; Schröder, N.; Glorius, F. *Adv. Synth. Catal.* **2014**, *356*, 1443−1460. (c) Song, G.; Li, X. *Acc. Chem. Res.* **2015**, *48*, 1007−1020.

(2) For a recent review see: (a) Satoh, T.; Miura, M. *Chem. - Eur. J.* **2010**, *16*, 11212−11222. (b) Song, G.; Wang, F.; Li, X. *Chem. Soc. Rev.* **2012**, *41*, 3651−3678. For recent representative examples of Rh(III)-catalyzed C−H activation in oxidative coupling reactions, see: (c) Pham, M. V.; Ye, B.; Cramer, N. *Angew. Chem., Int. Ed.* **2012**, *51*, 10610−10614. (d) Unoh, Y.; Hashimoto, Y.; Takeda, D.; Hirano, K.; Satoh, T.; Miura, M. *Org. Lett.* **2013**, *15*, 3258−3261. (e) Park, S.; Seo, B.; Shin, S.; Son, J. Y.; Lee, P. H. *Chem. Commun.* **2013**, *49*, 8671−8673. (f) Dong, Y.; Liu, G. *Chem. Commun.* **2013**, *49*, 8066−8068. (g) Dong, J.; Long, Z.; Song, F.; Wu, N.; Guo, Q.; Lan, J.; You, J. *Angew. Chem., Int. Ed.* **2013**, *52*, 580−584. (h) Itoh, M.; Hirano, K.; Satoh, T.; Shibata, Y.; Tanaka, K.; Miura, M. *J. Org. Chem.* **2013**, *78*, 1365−1370. (i) Liu, B.; Fan, Y.; Gao, Y.; Sun, C.; Xu, C.; Zhu, J. *J. Am. Chem. Soc.* **2013**, *135*, 468−473. (j) Muralirajan, K.; Cheng, C.-H. *Chem. - Eur. J.* **2013**, *19*, 6198−6202. (k) Qi, Z.; Li, X. *Angew. Chem., Int. Ed.* **2013**, *52*, 8995−9000. (l) Zhao, D.; Wu, Q.; Huang, X.; Song, F.; Lv, T.; You, J. *Chem. - Eur. J.* **2013**, *19*, 6239−6244. (m) Ghorai, D.; Choudhury, J. *Chem. Commun.* **2014**, *50*, 15159−15162. (n) Zheng, L.; Hua, R. *J. Org. Chem.* **2014**, *79*, 3930−3936. (o) Jayakumar, J.; Parthasarathy, K.; Chen, Y. H.; Lee, T. H.; Chuang, S. C.; Cheng, C. H. *Angew. Chem., Int. Ed.* **2014**, *53*, 9889−9892. (p) Iitsuka, T.; Hirano, K.; Satoh, T.; Miura, M. *Chem. - Eur. J.* **2014**, *20*, 385−389. (q) Qi, Z. S.; Wang, M.; Li, X. W. *Chem. Commun.* **2014**, *50*, 9776−9778. (r) Sun, H.; Wang, C.; Yang, Y.-F.; Chen, P.; Wu, Y.-D.; Zhang, X.; Huang, Y. *J. Org. Chem.* **2014**, *79*, 11863−11872. (s) Seoane, A.; Casanova, N.; Quiñones, N.; Mascareñas, J. L.; Gulías, M. *J. Am. Chem. Soc.* **2014**, *136*, 834−837. (t) Seoane, A.; Casanova, N.; Quinones, N.; Mascarenas, J. L.; Gulias, M. *J. Am. Chem. Soc.* **2014**, *136*, 7607−7610. (u) Pham, M. V.; Cramer, N. *Angew. Chem., Int. Ed.* **2014**, *53*, 3484−3487. (v) Qi, Z.; Yu, S.; Li, X. *J. Org. Chem.* **2015**, *80*, 3471−3479. (w) Ghorai, D.; Choudhury, J. *ACS Catal.* **2015**, *5*, 2692−2696. (x) Qin, D.; Wang, J.; Qin, X.; Wang, C.; Gao, G.; You, J. *Chem. Commun.* **2015**, *51*, 6190−6193. (y) Zhang, X.-S.; Zhang, Y.-F.; Li, Z.-W.; Luo, F.-X.; Shi, Z.-J. *Angew. Chem., Int. Ed.* **2015**, *54*, 5478−5482.

(3) (a) Guimond, N.; Gouliaras, C.; Fagnou, K. *J. Am. Chem. Soc.* **2010**, *132*, 6908−6909. (b) Guimond, N.; Gorelsky, S. I.; Fagnou, K. *J. Am. Chem. Soc.* **2011**, *133*, 6449−6457.

(4) (a) Rakshit, S.; Grohmann, C.; Besset, T.; Glorius, F. *J. Am. Chem. Soc.* **2011**, *133*, 2350−2353. (b) Wang, H.; Glorius, F. *Angew. Chem., Int. Ed.* **2012**, *51*, 7318−7322. (c) Wang, H.; Grohmann, C.; Nimphius, C.; Glorius, F. *J. Am. Chem. Soc.* **2012**, *134*, 19592−19595. (d) Zhao, D.; Shi, Z.; Glorius, F. *Angew. Chem., Int. Ed.* **2013**, *52*, 12426−12429.

(5) (a) Huang, H.; Ji, X.; Wu, W.; Jiang, H. *Chem. Soc. Rev.* **2015**, *44*, 1155−1171. (b) Patureau, F. W.; Glorius, F. *Angew. Chem., Int. Ed.* **2011**, *50*, 1977−1979.

(6) (a) Too, P. C.; Wang, Y.-F.; Chiba, S. *Org. Lett.* **2010**, *12*, 5688−5691. (b) Zhang, X.; Chen, D.; Zhao, M.; Zhao, J.; Jia, A.; Li, X. *Adv. Synth. Catal.* **2011**, *353*, 719−723. (c) Hyster, T. K.; Rovis, T. *Chem. Commun.* **2011**, *47*, 11846−11848. (d) Huckins, J. R.; Bercot, E. A.; Thiel, O. R.; Hwang, T.-L.; Bio, M. M. *J. Am. Chem. Soc.* **2013**, *135*, 14492−14495. (e) Zhou, B.; Hou, W.; Yang, Y.; Li, Y. *Chem. - Eur. J.* **2013**, *19*, 4701−4706. (f) Parthasarathy, K.; Cheng, C.-H. *J. Org. Chem.* **2009**, *74*, 9359−9364. (g) Parthasarathy, K.; Cheng, C.-H. *Synthesis* **2009**, *2009*, 1400−1402. (h) Parthasarathy, K.; Jeganmohan, M.; Cheng, C.-H. *Org. Lett.* **2008**, *10*, 325−328.

(7) (a) Chuang, S.-C.; Gandeepan, P.; Cheng, C.-H. *Org. Lett.* **2013**, *15*, 5750−5753. (b) Zheng, L.; Hua, R. *Chem. - Eur. J.* **2014**, *20*, 2352−2356. (c) Han, W. J.; Zhang, G. Y.; Li, G. X.; Huang, H. M. *Org. Lett.* **2014**, *16*, 3532−3535. (d) Muralirajan, K.; Cheng, C.-H. *Adv. Synth. Catal.* **2014**, *356*, 1571−1576. (e) Huang, X.-C.; Yang, X.-H.; Song, R.-J.; Li, J.-H. *J. Org. Chem.* **2014**, *79*, 1025−1031. (f) Su, B.; Wei, J.-b.; Wu, W.-l.; Shi, Z.-j. *ChemCatChem* **2015**, *7*, 2986−2990.

(8) (a) Shen, Y.; Liu, G.; Zhou, Z.; Lu, X. *Org. Lett.* **2013**, *15*, 3366−3369. (b) Liu, G.; Shen, Y.; Zhou, Z.; Lu, X. *Angew. Chem., Int. Ed.* **2013**, *52*, 6033−6037. (c) Zhang, H.; Wang, K.; Wang, B.; Yi, H.; Hu, F.; Li, C.; Zhang, Y.; Wang, J. *Angew. Chem., Int. Ed.* **2014**, *53*, 13234−13238. (d) Chen, Y.; Wang, D.; Duan, P.; Ben, R.; Dai, L.; Shao, X.; Hong, M.; Zhao, J.; Huang, Y. *Nat. Commun.* **2014**, *5*, 4610. (e) Hu, F.; Xia, Y.; Ye, F.; Liu, Z.; Ma, C.; Zhang, Y.; Wang, J. *Angew. Chem., Int. Ed.* **2014**, *53*, 1364−1367.

(9) (a) Huang, X.; Huang, J.; Du, C.; Zhang, X.; Song, F.; You, J. *Angew. Chem., Int. Ed.* **2013**, *52*, 12970−12974. (b) Zhang, X.; Qi, Z.; Li, X. *Angew. Chem., Int. Ed.* **2014**, *53*, 10794−10798. (c) Sharma, U.; Park, Y.; Chang, S. *J. Org. Chem.* **2014**, *79*, 9899−9906. (d) Dateer, R. B.; Chang, S. *J. Am. Chem. Soc.* **2015**, *137*, 4908−4911. (e) Kong, L.; Xie, F.; Yu, S.; Qi, Z.; Li, X. *Chin. J. Catal.* **2015**, *36*, 925−932. (f) Zhou, Z.; Liu, G.; Chen, Y.; Lu, X. *Adv. Synth. Catal.* **2015**, *357*, 2944−2950. (g) Zhou, B.; Chen, Z.; Yang, Y.; Ai, W.; Tang, H.; Wu, Y.; Zhu, W.; Li, Y. *Angew. Chem., Int. Ed.* **2015**, *54*, 12121−12126.

(10) (a) Liu, B.; Song, C.; Sun, C.; Zhou, S.; Zhu, J. *J. Am. Chem. Soc.* **2013**, *135*, 16625−16631. (b) Wang, C.; Huang, Y. *Org. Lett.* **2013**, *15*, 5294−5297. (c) Chen, J.; Chen, P.; Song, C.; Zhu, J. *Chem. - Eur. J.* **2014**, *20*, 14245−14249.

(11) Wen, J.; Wu, A.; Chen, P.; Zhu, J. *Tetrahedron Lett.* **2015**, *56*, 5282−5286.

(12) Yu, S.; Liu, S.; Lan, Y.; Wan, B.; Li, X. *J. Am. Chem. Soc.* **2015**, *137*, 1623−1631.

(13) Zhang, Q.-R.; Huang, J.-R.; Zhang, W.; Dong, L. *Org. Lett.* **2014**, *16*, 1684−1687.

(14) (a) Zhang, T.; Wu, L.; Li, X. *Org. Lett.* **2013**, *15*, 6294−6297. (b) Wangweerawong, A.; Bergman, R. G.; Ellman, J. A. *J. Am. Chem. Soc.* **2014**, *136*, 8520−8523. (c) Zhao, P.; Wang, F.; Han, K.; Li, X. *Org. Lett.* **2012**, *14*, 5506−5509. (d) Yadav, M. R.; Rit, R. K.; Sahoo, A. K. *Org. Lett.* **2013**, *15*, 1638−1641. (e) Huang, J. R.; Song, Q.; Zhu, Y. Q.; Qin, L.; Qian, Z. Y.; Dong, L. *Chem. - Eur. J.* **2014**, *20*, 16882−16886. (f) Hung, C.-H.; Gandeepan, P.; Cheng, C.-H. *ChemCatChem* **2014**, *6*, 2692−2697. (g) Dong, L.; Qu, C.-H.; Huang, J.-R.; Zhang, W.; Zhang, Q.-R.; Deng, J.-G. *Chem. - Eur. J.* **2013**, *19*, 16537−16540.

(15) (a) Neely, J. M.; Rovis, T. *J. Am. Chem. Soc.* **2014**, *136*, 2735−2738. (b) Neely, J. M.; Rovis, T. *J. Am. Chem. Soc.* **2013**, *135*, 66−69. (c) Zhao, D.; Lied, F.; Glorius, F. *Chem. Sci.* **2014**, *5*, 2869−2873. (d) Romanov-Michailidis, F.; Sedillo, K. F.; Neely, J. M.; Rovis, T. *J. Am. Chem. Soc.* **2015**, *137*, 8892−8895.

(16) CCDC 1414094 (**3ed**) contains supplementary crystallographic data for this paper.

(17) For selected examples on Rh(III)-catalyzed C−H activation and coupling with olefins for the constructions of five-membered heterocycles, see: (a) Ueura, K.; Satoh, T.; Miura, M. *Org. Lett.* **2007**, *9*, 1407−1409. (b) Shi, Z.; Schröder, N.; Glorius, F. *Angew. Chem., Int. Ed.* **2012**, *51*, 8092−8096. (c) Kim, D.-S.; Seo, Y.-S.; Jun, C.-H. *Org. Lett.* **2015**, *17*, 3842−3845. (d) Zhao, D.; Vásquez-Céspedes, S.; Glorius, F. *Angew. Chem., Int. Ed.* **2015**, *54*, 1657−1661. (e) Wang, F.; Song, G.; Li, X. *Org. Lett.* **2010**, *12*, 5430−5433. (f) Cajaraville, A.; López, S.; Varela, J. A.; Saá, C. *Org. Lett.* **2013**, *15*, 4576−4579.

(18) (a) Shi, X.-Y.; Li, C.-J. *Org. Lett.* **2013**, *15*, 1476−1479. (b) Shi, Z.; Boultadakis-Arapinis, M.; Glorius, F. *Chem. Commun.* **2013**, *49*,

DOI: 10.1021/acscatal.5b02297
ACS Catal. 2016, 6, 1971−1980

6489−6491. (c) Zuo, Z.; Yang, X.; Liu, J.; Nan, J.; Bai, L.; Wang, Y.; Luan, X. *J. Org. Chem.* **2015**, *80*, 3349−3356. (d) Sueki, S.; Kuninobu, Y. *Chem. Commun.* **2015**, *51*, 7685−7688. For an early example of Re-catalyzed synthesis of indenes via C−H activation, see: (e) Kuninobu, Y.; Kawata, A.; Takai, K. *J. Am. Chem. Soc.* **2005**, *127*, 13498−13499.

(19) For examples of using maleimides as a coupling partner in C−H activation, see: (a) Kiyooka, S.-i.; Takeshita, Y. *Tetrahedron Lett.* **2005**, *46*, 4279−4282. (b) Nishino, M.; Hirano, K.; Satoh, T.; Miura, M. *J. Org. Chem.* **2011**, *76*, 6447−6451. (c) Wang, F.; Song, G.; Du, Z.; Li, X. *J. Org. Chem.* **2011**, *76*, 2926−2932. (d) Zhang, T.; Qi, Z.; Zhang, X.; Wu, L.; Li, X. *Chem. - Eur. J.* **2014**, *20*, 3283−3287. (e) Miura, W.; Hirano, K.; Miura, M. *Org. Lett.* **2015**, *17*, 4034−4037.

(20) (a) Popowycz, F.; Routier, S.; Joseph, B.; Mérour, J.-Y. *Tetrahedron* **2007**, *63*, 1031−1064. (b) Mérour, J.-Y.; Joseph, B. *Curr. Org. Chem.* **2001**, *5*, 471−506.

(21) Frisch, M. J.; Trucks, G. W.; Schlegel, H. B.; Scuseria, G. E.; Robb, M. A.; Cheeseman, J. R.; Scalmani, G.; Barone, V.; Mennucci, B.; Petersson, G. A.; Nakatsuji, H.; Caricato, M.; Li, X.; Hratchian, H. P.; Izmaylov, A. F.; Bloino, J.; Zheng, G.; Sonnenberg, J. L.; Hada, M.; Ehara, M.; Toyota, K.; Fukuda, R.; Hasegawa, J.; Ishida, M.; Nakajima, T.; Honda, Y.; Kitao, O.; Nakai, H.; Vreven, T.; Montgomery, J. A., Jr.; Peralta, J. E.; Ogliaro, F.; Bearpark, M.; Heyd, J. J.; Brothers, E.; Kudin, K. N.; Staroverov, V. N.; Keith, T.; Kobayashi, R.; Normand, J.; Raghavachari, K.; Rendell, A.; Burant, J. C.; Iyengar, S. S.; Tomasi, J.; Cossi, M.; Rega, N.; Millam, J. M.; Klene, M.; Knox, J. E.; Cross, J. B.; Bakken, V.; Adamo, C.; Jaramillo, J.; Gomperts, R.; Stratmann, R. E.; Yazyev, O.; Austin, A. J.; Cammi, R.; Pomelli, C.; Ochterski, J. W.; Martin, R. L.; Morokuma, K.; Zakrzewski, V. G.; Voth, G. A.; Salvador, P.; Dannenberg, J. J.; Dapprich, S.; Daniels, A. D.; Farkas, O.; Foresman, J. B.; Ortiz, J. V.; Cioslowski, J.; and Fox, D. J. *Gaussian 09, revision D.01*; Gaussian, Inc., Wallingford, CT, 2013.

(22) (a) Becke, A. D. *J. Chem. Phys.* **1993**, *98*, 5648−5652. (b) Lee, C.; Yang, W.; Parr, R. G. *Phys. Rev. B: Condens. Matter Mater. Phys.* **1988**, *37*, 785−789.

(23) Peverati, R.; Truhlar, D. G. *J. Phys. Chem. Lett.* **2012**, *3*, 117−124.

(24) (a) Peverati, R.; Truhlar, D. G. *Phys. Chem. Chem. Phys.* **2012**, *14*, 11363−11370. (b) Lin, Y.-S.; Tsai, C.-W.; Li, G.-D.; Chai, J.-D. *J. Chem. Phys.* **2012**, *136*, 154109. (c) Steckel, J. A. *J. Phys. Chem. A* **2012**, *116*, 11643−11650. (d) Zhao, Y.; Ng, H. T.; Peverati, R.; Truhlar, D. G. *J. Chem. Theory Comput.* **2012**, *8*, 2824−2834. (e) Yu, Z.; Lan, Y. *J. Org. Chem.* **2013**, *78*, 11501−11507. (f) Long, R.; Huang, J.; Shao, W.; Liu, S.; Lan, Y.; Gong, J.; Yang, Z. *Nat. Commun.* **2014**, *5*, 5707.

(25) Marenich, A. V.; Cramer, C. J.; Truhlar, D. G. *J. Phys. Chem. B* **2009**, *113*, 6378−6396.

(26) (a) Li, L.; Brennessel, W. W.; Jones, W. D. *Organometallics* **2009**, *28*, 3492−3500. (b) Zhang, Q.; Yu, H.-Z.; Li, Y.-T.; Liu, L.; Huang, Y.; Fu, Y. *Dalton Trans.* **2013**, *42*, 4175−4184. (c) Zhang, X.-S.; Chen, K.; Shi, Z.-J. *Chem. Sci.* **2014**, *5*, 2146−2159. (d) Liu, L.; Wu, Y. L.; Wang, T.; Gao, X.; Zhu, J.; Zhao, Y. F. *J. Org. Chem.* **2014**, *79*, 5074−5081. (e) Chen, W.-J.; Lin, Z. *Organometallics* **2015**, *34*, 309−318. (f) Yu, S.; Liu, S.; Lan, Y.; Wan, B.; Li, X. *J. Am. Chem. Soc.* **2015**, *137*, 1623−1631. (g) Li, Y.; Liu, S.; Qi, Z.; Qi, X.; Li, X.; Lan, Y. *Chem. - Eur. J.* **2015**, *21*, 10131−10137.

DOI: 10.1021/acscatal.5b02297
ACS Catal. 2016, 6, 1971−1980